

Research Article

An Alcohol-Free SiO₂ Sol-Gel Matrix Functionalized with Acetic Acid as Drug Reservoir for the Controlled Release of Pentoxifylline

Mayra Angélica Alvarez Lemus,¹ Oscar Javier Ortiz Castañeda,¹
Alma Delia Hernández Pérez,² and Rosendo López González¹

¹ *División Académica de Ingeniería y Arquitectura, Universidad Juárez Autónoma de Tabasco, Carr. Cunduacán-Jalpa de Méndez Km. 1, Colonia La Esmeralda, 86690 Cunduacán, TAB, Mexico*

² *Laboratorio de Microscopía Electrónica, Instituto Nacional de Rehabilitación, Calz. México-Xochimilco 289, Colonia Arenal de Guadalupe, 14389 Tlalpan, D.F., Mexico*

Correspondence should be addressed to Mayra Angélica Alvarez Lemus; mayra.alvarez@ujat.mx

Received 14 March 2014; Revised 22 May 2014; Accepted 22 May 2014; Published 6 July 2014

Academic Editor: Zhongkui Hong

Copyright © 2014 Mayra Angélica Alvarez Lemus et al. This is an open access article distributed under the Creative Commons Attribution License, which permits unrestricted use, distribution, and reproduction in any medium, provided the original work is properly cited.

Pentoxifylline (PTX) is a xanthine derivative, with hemorrheologic properties, that has been useful in the treatment of several diseases. However, a conventional route of administration implies high doses, what is unnecessary to the organism, seriously increasing the risk of toxicity because of side effects. Because of the facility to modify their surface, sol-gel materials have proved to be suitable reservoirs for a variety of molecules for biological applications. In this work we prepared alcohol-free SiO₂ material by the sol-gel process using acetic acid as surface modifier and hydrolysis catalyst, the alkoxide/water ratio (R_w) used was 1/16, and tetraethylorthosilicate was used as SiO₂ precursor. Spectroscopic characterization was carried out by means of FTIR-ATR and UV-Visible spectroscopies; the results confirmed the presence of the drug and interactions between sol-gel matrix and PTX. BET specific surface area values of the sol-gel materials were 365 and 462 m²/g for SiO₂ and PTX-SiO₂, respectively. Synthesized SiO₂ nanoparticles showed efficient entrapment of PTX since a controlled release of 83% of drug content was reached.

1. Introduction

3,7-Dihydro-3,7-dimethyl-1-(5-oxohexyl)-1H-purine-2,6-dione or pentoxifylline (PTX), a trisubstituted xanthine derivative, is a hemorrheologic [1, 2] and anti-inflammatory drug that is known to prevent immune cells from producing inflammatory cytokines [3]. This drug improves blood flow by increasing deformation capability of erythrocytes, reducing leucocytes adherence to endothelium, diminishes erythrocytes and platelets aggregation (antithrombotic) [4], and decreases fibrinogen levels [5, 6]. PTX is used to increase circulation in patients with peripheral arterial disease (PAD) [7] and in several vascular disorders, nonalcoholic steatohepatitis, and also in patients with angina pectoris and venous leg ulcers while recent applications of PTX include fibrosis and erectile dysfunction [8, 9]. PTX is readily

absorbed (up to 95%) from the gastrointestinal tract, but undergoes extensive first pass hepatic metabolism (60–70%) [10]; administrations of this drug are associated with some effects, gastrointestinal side effects being the most common including nausea, vomiting, gas, and belching. Nervous system side effects have occurred in 1% to 2% of treated patients and have included headache, insomnia, tremor, and dizziness [11]. Cardiovascular side effects have included reports of palpitations, flushing, and angina. These reports have usually been associated with higher doses of an immediate release.

Due to its numerous benefits, some attempts have been made to improve the efficiency of the drug by encapsulation [12]. Novel formulations for controlled drug delivery have become one of the most explored fields worldwide, since different diseases could be efficiently treated by means of this approach. The use of organic polymers [13] or liposomes [3]

has been explored during the last years; however this type of formulations shows low encapsulation efficiencies with release percentages varying from 50 to 90%. One of the main successful trends in this field is local application of therapeutics using nanoparticles since it represents an alternative to increasing drug concentrations in target organs or tissues [14]. Obtaining of drug-loaded nanomaterials has gained attention in nanomedicine, and their design represents a challenge in order to find the most suitable host nanomaterial for specific drug properties.

Surface modification of materials allows enhancing or improving adsorption of molecules of interest like drugs, enzymes, or antibodies just to mention a few. For controlled release purposes, the main goal is to entrap inside a nanostructured reservoir, lower drug doses than those used by systemic administration, to prevent adverse side effects, whereas nanomaterial acts as reservoir and shield protecting the drug from physiological conditions increasing therapeutic effect in target sites. Currently, there are several ways to modify nanomaterials surface as well as a variety of anchorable functional groups. Among most commonly used, hydroxyl groups through different precursors have gained interest. It has been reported that oxygen-containing functional groups are very good applicants to bind to the silicon surface, because of the strong Si–O bond [15]. Sol-gel materials have highly hydroxylated surface, also this method is suitable for in situ surface modification, by adding functionalizing agents either at the first stage or once the gel was obtained.

In the development of more efficient biomaterials, surface modification is currently one of the most useful techniques since this improves their properties. For this purpose, several chemicals are under current investigation, –COOH, –SH, and –NH₂ being the most popular [16]. In our work we used acetic acid which possesses a –COOH functional group and is a weak acid with particular behavior at physiological pH; moreover acetic acid has showed antibacterial and antifungal properties. Its biological role discovered by biochemist Konrad Emil Bloch as the primary precursor in the production of body cholesterol and its antimicrobial properties [17] make it suitable for biological applications.

In this research, we incorporated PTX in an alcohol-free SiO₂ nanostructured matrix for controlled release purposes; together with SiO₂ as reference, the samples were characterized by several physical techniques. Drug release profiles were recorded by UV-Vis spectroscopy and kinetic analysis was carried out by fitting data to zero and first order mathematical models.

2. Materials and Methods

2.1. Synthesis. 5 g of SiO₂ and PTX-SiO₂ were prepared by the sol-gel process. Tetraethylorthosilicate (TEOS, SIGMA-ALDRICH 98%) was used as silicon oxide precursor. Alkoxide-water molar ratio was 1 : 16. In order to functionalize materials surface, acetic acid (REASOL, 99.7%) was used by adding 3 mL of a 0.1 M acetic acid solution to distilled water until pH 3 was reached. For PTX-SiO₂ material, same procedure was used with addition of 200 mg of PTX. TEOS was added slowly and the mixture was kept under continuous

stirring until gel formation. The sols were maintained under continuous stirring at room temperature until the gel was formed; then the samples were dried and milled for further analysis.

2.2. Sample Characterization

2.2.1. Infrared ATR Spectroscopy. The powders were mixed with KBr (95%) and pressed into a CARNER pellet mill. The wafers were analyzed in an IR Affinity-1 (Shimadzu) spectrometer in Absorbance mode.

2.2.2. UV-Visible Spectroscopy. For diffuse reflectance measurements an UV-Vis spectrophotometer (Varian, Cary-100) with integrating sphere attachment DRA-CA-30I was used. The equipment was calibrated using Spectralon standard (Labsphere SRS-99-010, 99% reflectance). The optical absorption was measured in the 200–800 nm range.

2.2.3. Scanning Electron Microscopy and Electron Dispersive Spectroscopy. SEM micrographs were taken with a JEOL JSM-6010LV microscope; microanalysis was carried out with a EDS Bruker equipment (QUANTAX system).

2.2.4. Transmission Electron Microscopy. Powder samples were mixed in ethanol and dispersed in an ultrasonic bath, after that a drop of this suspension was deposited in a carbon covered copper grid and then observed in the microscope to further analysis. Transmission electron microscopy was performed in a Philips (FEI) Tecnai 10 at accelerating voltage of 80 kV attached to MegaView III camera (SIS).

2.2.5. Thermal Analysis. Thermogravimetric analysis (TGA) and differential scanning calorimetry (DSC) graphics were obtained in a STA i-1000 thermal analyzer, 10 cm³ /min with N₂ flux from room temperature to 800 °C.

2.2.6. N₂ Adsorption. Samples were degassed at 50 °C during 48 hours in a Bellprep II station, and then the samples were analyzed in a Bellsorp II equipment, at 77 K using N₂ as adsorptive. Surface area was calculated by the Brunauer-Emmet-Teller (BET) method and pore size distributions were obtained from desorption isotherms using Barret, Joyner, and Halenda (BJH) method.

2.3. In Vitro Pentoxifylline Release. 100 mg of PTX-SiO₂ was pressed to obtain thin disks with diameter of 1 cm. Each wafer was placed into a flask containing distilled water (100 ml). Samples of supernatant (ca. 3 mL) were collected to obtain UV-Vis spectra at regular intervals of time and returned to the flask to keep constant volume. Drug release profiles were obtained by following the main absorption band of PTX (274 nm). A calibration curve was made and concentration of the samples at time *t* was obtained applying Beer-Lambert law.

3. Results

3.1. Sample Characterization. Collected infrared spectra are shown in Figure 1. In the 4000–2750 cm⁻¹ region, we observed a broad band for PTX-SiO₂ and SiO₂ materials that

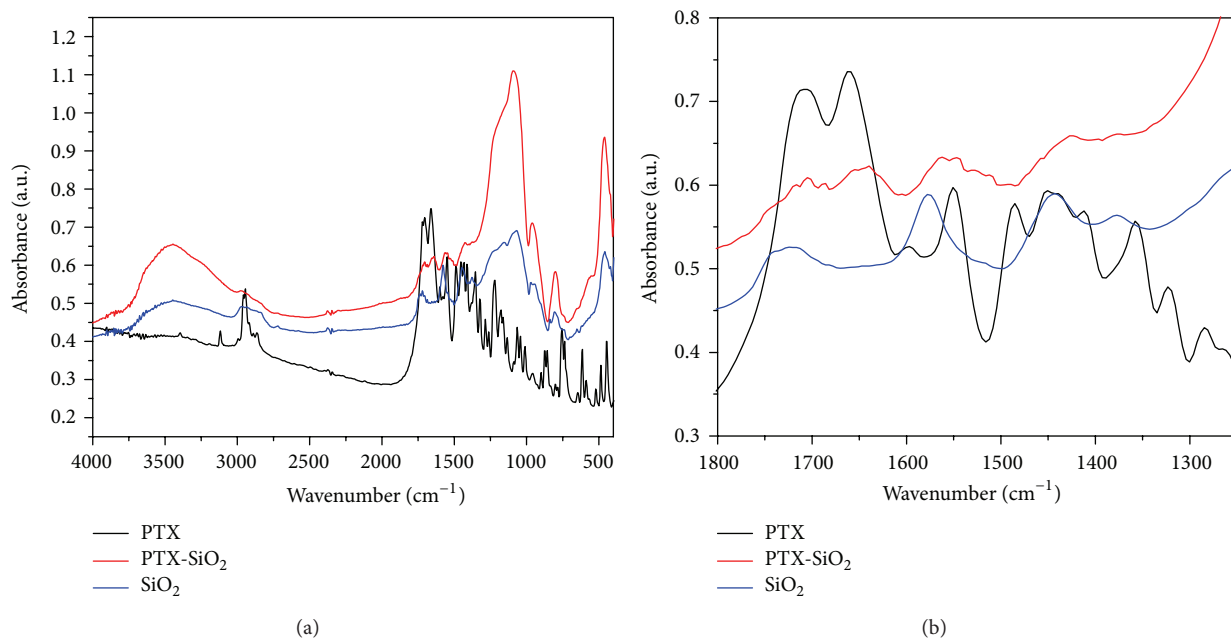


FIGURE 1: ATR-FTIR spectra of the materials. (a) Full range and (b) mid-energy region.

corresponds to O–H stretching and Si–OH vibrations; around 2960 cm⁻¹ the presence of C–H vibrations from PTX and acetic acid is clearly evidenced. Two characteristic bands of PTX are located at 1720 and 1705 cm⁻¹ and one at 1658 cm⁻¹; these can be assigned to –CO stretching and amide –CO stretching mode vibrations. These bands appear with lower intensity in the PTX-SiO₂ spectra indicating that the drug is interacting with SiO₂, whereas in SiO₂ only appears the band at 1724 cm⁻¹ that can be associated with the presence of acetic acid. In PTX-SiO₂ spectrum corresponding bands to Si–O–Si asymmetric stretching vibration are located at 1222 and 1091 cm⁻¹, together with that observed at 798 cm⁻¹ which corresponds to symmetric stretching [18, 19], and the band usually presented in xerogels due to Si–OH stretching appears at 956 cm⁻¹. Finally the band that appears around 455 cm⁻¹ also is commonly found in xerogels and is related to the presence of network defects such as tetra or trisiloxane rings. Regarding SiO₂ sample, the above-mentioned bands due to Si–O–Si and Si–OH bands were observed too. In the region between 1680 and 1750 cm⁻¹ we observed a broad band in pure SiO₂ and PTX-SiO₂ samples around 1724 cm⁻¹; this band is associated with the carbonyl group and its presence in SiO₂ sample can be due to incorporation of acetic acid, as well as that observed in 2835–2974 cm⁻¹ attributable to C–H vibrations. With these results we can assume the presence of both compounds PTX and acetic acid in PTX-SiO₂ and acetic acid in SiO₂ samples.

In order to analyze the effect of PTX in SiO₂, UV-absorbance spectra of all the materials were normalized using Origin 8.0 (Figure 2). The main band of PTX has been reported at 274 nm [3, 20, 21] and corresponds to $n \rightarrow \pi^*$ transitions. We collected the spectrum of a PTX solution (0.002 mg/mL), where we observed the band at 274 nm and

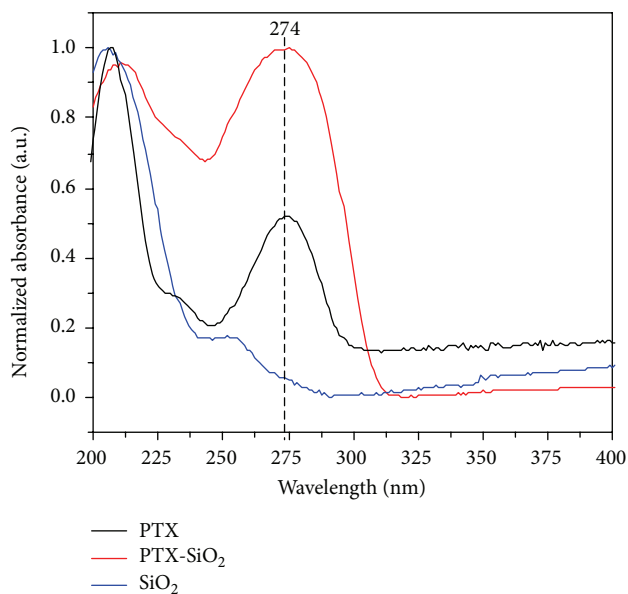


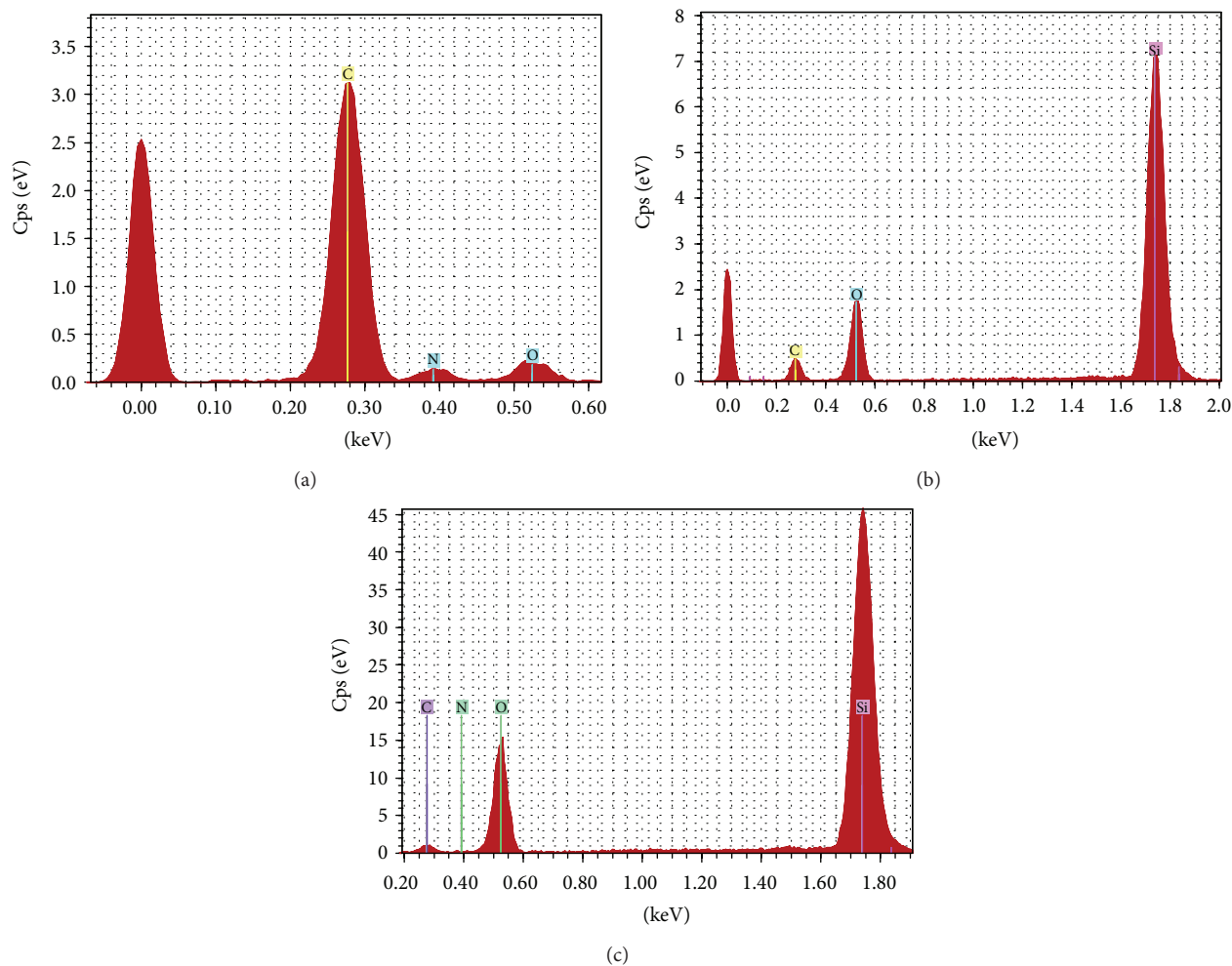
FIGURE 2: Normalized UV absorption spectra of SiO₂, PTX, and PTX-SiO₂. Dotted line indicates the main absorption band of PTX.

the other one centered at 207 nm due to $\pi \rightarrow \pi^*$ transitions. In SiO₂ spectrum two absorption bands were observed, the first one located at 206 nm corresponds to electronic transitions exhibited by sol-gel SiO₂ materials; while the other (254 nm) can be assigned to the presence of acetate groups on the surface of SiO₂ which main absorption bands have been reported at 204 and 260 nm.

Electron dispersive spectroscopy of three samples is shown in Figure 3. We observed the presence of high

TABLE 1: Elemental analysis by electron dispersive spectroscopy (EDS) of the sample PTX-SiO₂.

Element	Atomic number	wt% (unnormalized)	wt% (normalized)	at%	Error wt% (1 sigma)
O	8	45.75	41.42	46.99	7.42
Si	14	44.84	40.60	26.23	1.97
C	6	17.84	16.15	24.40	4.86
N	7	2.03	1.83	2.38	1.22

FIGURE 3: Electron dispersive spectroscopy of (a) bare PTX and (b) PTX-acetic acid-SiO₂ and (c) SiO₂. Elemental composition of particles surface is provided where carbon, nitrogen silicon, and oxygen can be detected.

concentrations of carbon and detected nitrogen and oxygen in the PTX analysis (Figure 3(a)). PTX-SiO₂ and SiO₂ are shown in Figures 3(b) and 3(c), respectively, where we observed the presence of the drug in SiO₂. Elemental analysis of the sample PTX-SiO₂ is shown in Table 1. Regarding morphological analysis scanning electron microscopy images showed PTX-SiO₂ smaller aggregates than those observed in SiO₂ (Figure 4).

Particle size of the samples is around 100 nm in pure silica; however formation of clumps made of nanoparticles can be observed from TEM (Figure 5). When PTX is incorporated into SiO₂, nanoparticles seemed to be less attached to each

other and single particles are clearly observed, but none exceeded 100 nm. Sol-gel process is an efficient technique to obtaining nanoparticles, with particular morphology influenced by the addition of the drug.

Figure 6 shows corresponding thermal analysis curves for all the samples. Anhydrous nature of PTX is evident in the lack of noticeable weight loss when the compound was heated as high as 211°C (inset). Beyond 250°C and up to 345°C an extensive weight loss was observed, which corresponds to exothermic decomposition of the drug. DSC endothermic peak at 111°C can be identified as melting transition of PTX [22]. We observed that SiO₂ has an endothermic weight loss

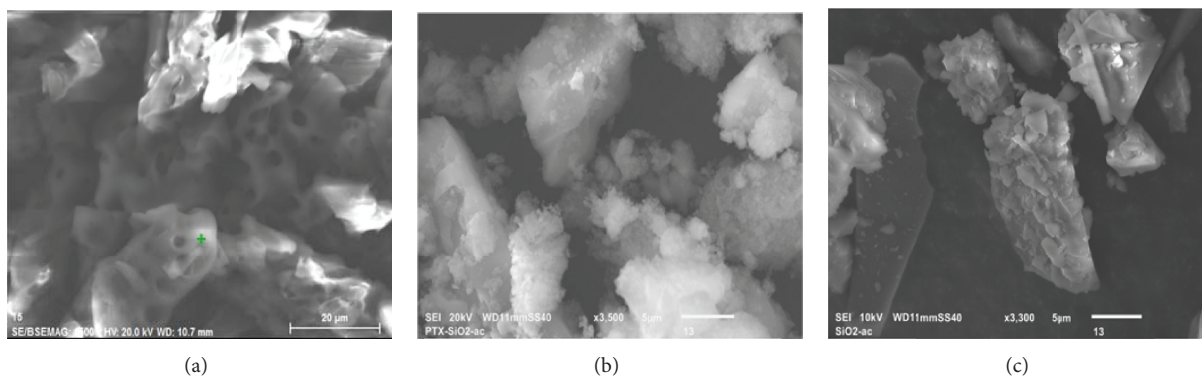


FIGURE 4: Scanning electron microscopy images of the samples. Particles bigger than $20\ \mu\text{m}$ correspond to pentoxifylline (a), while inclusion of the drug in the functionalized SiO_2 modifies the surface morphology and size (b). For SiO_2 aggregates of different sizes were observed (c).

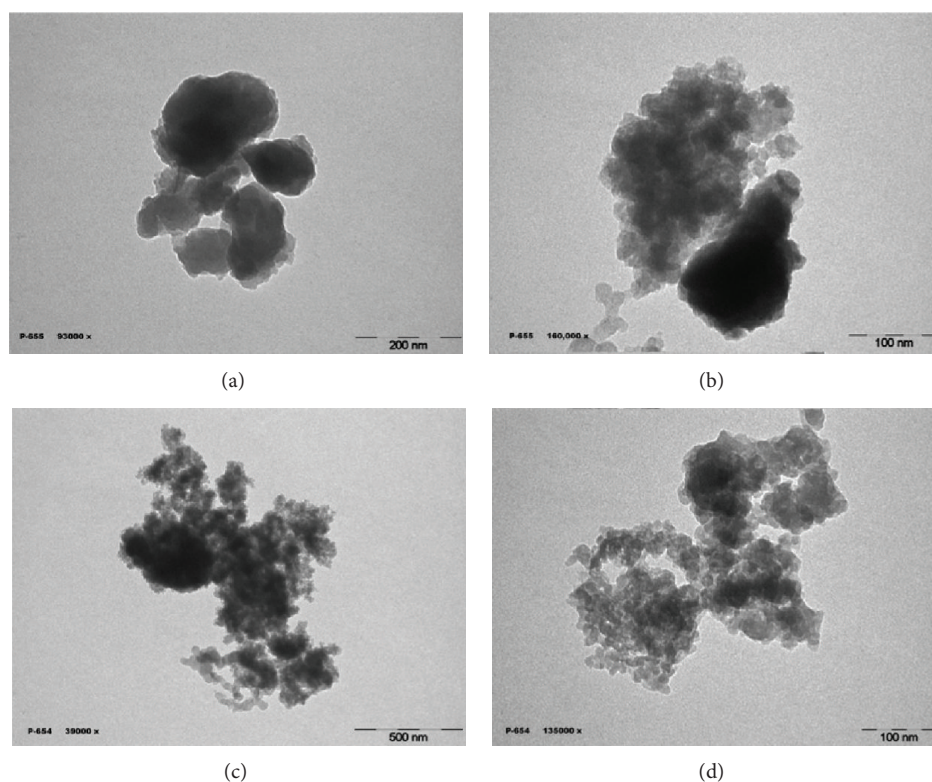
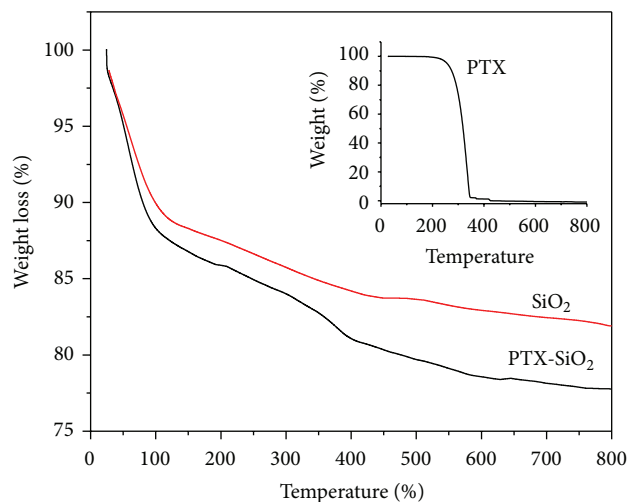


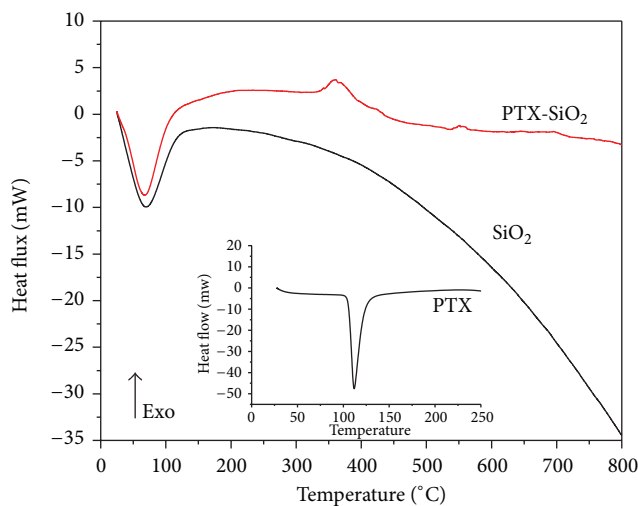
FIGURE 5: Transmission electron microscopy images of acetic acid- SiO_2 (a), (b) and PTX-acetic acid- SiO_2 (c), (d).

of ca. 16% in the temperature range from 25°C to 110°C , which is mainly associated with thermal removal of adsorbed water and acetic acid. This signal is followed by a broad region of weight loss that corresponds with dehydroxylation process of silica. It is important to note that no exothermic peaks were observed in the $120\text{--}800^\circ\text{C}$ range, which indicates that the sample does not crystallize. Nevertheless, this thermal behavior is different from that observed in PTX- SiO_2 sample, where we observed a higher weight loss than in SiO_2 in the $118\text{--}380^\circ\text{C}$ region (about 3%), and is associated with a small exothermic peak centered at 334°C that is in agreement with reported thermal decomposition of PTX and close to the nominal concentration of the drug.

With the aim of determining BET surface area and BJH pore distribution we used N_2 adsorption desorption isotherms (Figure 7). We observed that when $p/p_0 < 0.2$, both materials SiO_2 and PTX- SiO_2 adsorbed almost the same volume; however above this value SiO_2 isotherm takes the form of reversible Type I isotherm (*Langmuir isotherm*), which is concave to the p/p_0 axis and approaches to a limiting value as $p/p_0 \rightarrow 1$. This type of isotherms is given by microporous solids with relatively small external surfaces; when PTX is incorporated to silica, adsorption behavior is completely different, since PTX- SiO_2 corresponding isotherm is Type II according to IUPAC, which is the normal form of isotherm observed in a nonporous or



(a)



(b)

FIGURE 6: (a) Thermogravimetric analysis and (b) differential scanning calorimetry curves of nanoparticles acetic acid-functionalized nanomaterials SiO_2 and PTX- SiO_2 . The inset shows thermogravimetric profile of bare PTX.

macroporous adsorbent. However, in our sample, this is associated with the coverage of silica by PTX molecules; hysteresis loop corresponds to type H3, which does not exhibit any limiting adsorption at high p/p_0 , commonly observed with aggregates of plate-like particles giving rise to slit-shaped pores. Regarding surface area and pore size distribution, we observed that PTX- SiO_2 exhibited a $S_{\text{BET}} = 462 \text{ m}^2/\text{g}$ while bare SiO_2 was $365 \text{ m}^2/\text{g}$. Although both samples showed the same value for mean pore diameter (2.4 nm) for PTX- SiO_2 we observed the presence of a considerable amount of pores between 4 and 8 nm.

3.2. Drug Release Profile. Controlled release of active principles has been one of the most investigated areas in pharmacology. In order to increase therapeutic effect, strategies like encapsulation or entrapment of a variety of drugs have

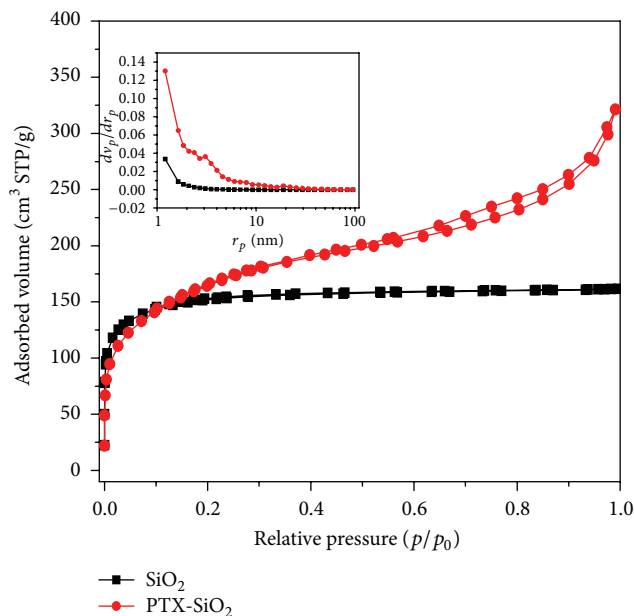


FIGURE 7: N_2 adsorption-desorption isotherms and pore size distribution (inset) of SiO_2 and PTX- SiO_2 samples.

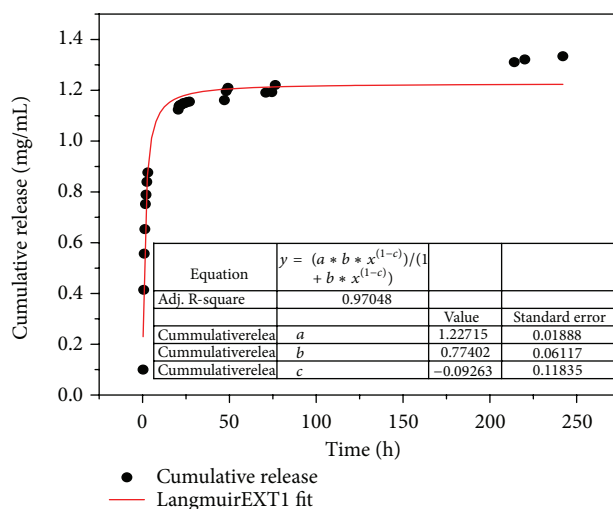


FIGURE 8: Cumulative release profile of PTX. The drug dissolutions were carried out in distilled water and analyzed by ultraviolet spectroscopy. Langmuir extended mathematical model was used.

been used to use low doses and minimize adverse side effects. We observed that, after several weeks, PTX remained unmodified, since no changes were observed in UV-Visible spectrum. When PTX release was monitored *in vitro*, cumulative drug amount versus time was plotted (Figure 8), and discharge of the drug takes place in two steps, where the initial takes place from $t = 0$ up to $t = 3 \text{ h}$, with a 24% released of the drug. In the following hours a slower profile was observed reaching the 83% after 250 h, which means that encapsulation yield was about 98% regarding the initial amount of PTX placed. We observed that obtained data showed a better fit when Langmuir extended model is applied

($r^2 = 0.97$) (1), whereas first order kinetics had $r^2 = 0.92$ and estimated constants for these two-step release profiles were 2.44 and 1.25, respectively (see Supplementary Material, available online at <http://dx.doi.org/10.1155/2014/853967>). These results showed the efficiency and usefulness of sol-gel silica as drug-reservoir. Consider

$$C = \frac{abt^{1-c}}{1 + bt^{1-c}}, \quad (1)$$

where a , b , and c are coefficients of the equation, C is the cumulative release (mg/mL), and t time (h).

4. Discussion

It is well known that hydroxyl groups of sol-gel materials bring special features to its surface. For drug release purposes, these groups provide major interaction between material surface and loaded drug. Also, the hydrogen bonds have enormous effect on uptake guest molecules. On the other hand, carboxylic groups have been demonstrated to be good enhancers for biocompatible and bioactive surfaces [23]. In this research we include in a sol-gel matrix of silicon dioxide both a drug and a surface modifier. FTIR spectroscopy characterization gave us evidence about interactions between PTX and surface OH groups from sol-gel SiO₂. Also, modifying surface of the SiO₂ nanoparticles was well observed. One of the most useful properties of sol-gel process is the facility for incorporation of a broad variety of molecules during the first stages of the process; additionally using low temperatures represents a suitable feature for entrapment of pharmacologically active compounds.

Acetic acid modified UV-Vis spectra of SiO₂ shifting its main absorption band toward higher energy are related to interactions between carbonyl group and hydrogen bonds formed with silica surface. Incorporation of PTX on silicon dioxide can be inferred due to the presence of an additional and intense band centered at 274 nm, which is not exhibited by SiO₂ material. The band corresponding to SiO₂ is shifted toward lower energy due to strong interactions between PTX, acetate group, and SiO₂. This can be supposed since acetate ions have the possibility to coordinate with silicon atoms through carboxylate group in three different ways: monodentate or bidentate or with acid-base pair sites [24].

It is well known that properties of pure silicon dioxide strongly depend on the chemical activity of its surface, determined by the concentration and distribution of OH groups, and the porous structure of the matrix [25]. Several studies on SiO₂ surface have been carried out and have proved that different types of amorphous SiO₂ contain not only OH groups on its surface, but also structurally bounded water within the matrix and even inside micropores of the sample. Thus, porosity plays an important role on SiO₂ surface behavior. Besides high concentrations of surface and structural OH groups, sol-gel materials commonly possess high surface area and microporosity.

As Figure 4(b) showed, incorporation of the drug in SiO₂ modified its surface which clearly differs from bare oxide. Water solubility of the drug facilitates its entrapment into

porous SiO₂; however drug size and microporosity of SiO₂ favor higher concentration of the drug on the external surface of SiO₂ than inside porous. This is related to the two-step release observed in the *in vitro* profile, since at the beginning the system delivered around 24% of entrapped drug whereas the remainder drug was released slower, and corresponds to the drug entrapped inside SiO₂ framework. This fact allowed a desirable progressive release, in order to avoid undesirable side effects caused by high local concentrations of PTX.

Due to the different applications of PTX in several diseases, some attempts have been made to encapsulate this drug in diverse matrices; however, until now, silica matrices have not been reported yet. Rahman and coworkers [20] found that when PTX is encapsulated in matrices of cellulose, the release was governed by the presence of microcrystals in cellulose; they obtained matrices with a 50–60% of encapsulation efficiency 65% released after 8 hours. Another research group who investigated use of scaffolds to avoid fibrous formation in biomedical implants reported similar efficiencies with releases of 60 to 90% in 1.5 hours when alginate-chitosan scaffolds are used [3]. Depending on the final destination of the drug-vehicle, different rates of release are required. In our work, we used the solid network of silica to entrap PTX to be used as slow-release vehicle with promising results.

5. Conclusions

Pentoxifylline is a drug with novel applications in therapeutics; however its side effects and low effect after repeated doses limit its potential. The use of different vehicles in order to improve therapeutic effect of drugs represents one of the most important fields of research in medicine. In this sense, nanoparticles of inorganic oxides can be easily fabricated with a wide variety of additives to enhance their surface properties, and particularly the sol-gel chemistry shows relative facility to control the synthesis variables, which allows designing materials for very specific applications, such as controlled release of drugs. Addition of acetic acid did not influence chemical structure of the drug since PTX was released without chemical modifications. In this work, addition of acetic acid has two different intentions: (1) to act as a functionalizing of SiO₂ surface and (2) as hydrolysis catalyst.

This PTX-SiO₂ functionalized system was characterized and evidences of drug-silica interaction were confirmed. Important features in this type of devices are porosity and surface area, since internal and external areas participate in adsorption of the drug, depending on its size and chemical structure. The obtained material exhibited large surface area with a well-defined pore size distribution, allowing entrapment of PTX molecules in two different ways: first by filling micropores and then adsorbing over the external surface. The drug release profile showed that silica particles represent a good alternative to entrap efficiently the desired amount of drug, with sustained and slow liberation during 25 h. Such a drug release profile at the active site can make the carrier a viable candidate for clinical application in wounds because

of the presence of the active principle, PTX, and acetic acid which could act as antimicrobial agent.

Conflict of Interests

The authors certify that they have no affiliations with or involvement in any organization or entity with any financial interest or nonfinancial interest in the subject matter or materials discussed in this paper.

Acknowledgments

The authors want to thank the Federal District Science and Technology Institute Project PIFUT80-130 for financial support and also National Institute of Neurology and Neurosurgery for facilities. The authors are deeply grateful to E. Amaro and T. López for Technical assistance and facilities, respectively, in SEM and EDS analysis.

References

- [1] National Cancer Institute, "NCI Drug Dictionary," 2012, <http://www.cancer.gov/drugdictionary>.
- [2] J. de Haro, F. Acin, A. Florez, S. Bleda, and J. L. Fernandez, "A prospective randomized controlled study with intermittent mechanical compression of the calf in patients with claudication," *Journal of Vascular Surgery*, vol. 51, no. 4, pp. 857–862, 2010.
- [3] H.-L. Lin and C.-T. Yeh, "Alginate-crosslinked chitosan scaffolds as pentoxifylline delivery carriers," *Journal of Materials Science: Materials in Medicine*, vol. 21, no. 5, pp. 1611–1620, 2010.
- [4] F. Bertocchi, P. Proserpio, M. G. Lampugnai, and E. Dejana, "The effect of pentoxifylline on polymorphonuclear cell adhesion to cultured endothelial cells," in *Pentoxifylline and Leukocyte Function*, G. L. Mandell and W. J. Novick, Eds., Hoechst-Roussel Pharmaceuticals, Somerville, NJ, USA, 1988.
- [5] P. E. M. Jarrett, M. Moreland, and N. L. Browse, "The effect of oxpentifylline (Trental[®]) on fibrinolytic activity and plasma fibrinogen levels," *Current Medical Research and Opinion*, vol. 4, no. 7, pp. 492–495, 1977.
- [6] H.-P. Llöcking, A. Hoffmann, and F. Markwardt, "Release of plasminogen activator by pentoxifylline and its major metabolite," *Thrombosis Research*, vol. 46, no. 5, pp. 747–750, 1987.
- [7] J. V. Mascarenhas, M. A. Albayati, C. P. Shearman, and E. B. Jude, "Peripheral arterial disease," *Endocrinology and Metabolism Clinics of North America*, vol. 43, no. 1, pp. 149–166, 2014.
- [8] M. Albersen, T. M. Fandel, H. Zhang et al., "Pentoxifylline promotes recovery of erectile function in a rat model of postprostatectomy erectile dysfunction," *European Urology*, vol. 59, no. 2, pp. 286–296, 2011.
- [9] M. Goicoechea, S. G. de Vinuesa, B. Quiroga et al., "Effects of pentoxifylline on inflammatory parameters in chronic kidney disease patients: a randomized trial," *Journal of Nephrology*, vol. 25, no. 6, pp. 969–975, 2012.
- [10] A. Chmielewska, L. Konieczna, A. Plenis, and H. Lamparczyk, "Quantitative determination of pentoxifylline in human plasma," *Acta Chromatographica*, no. 16, pp. 70–79, 2006.
- [11] A. Ward and S. P. Clissold, "Pentoxifylline: a review of its pharmacodynamic and pharmacokinetic properties, and its therapeutic efficacy," *Drugs*, vol. 34, no. 1, pp. 50–97, 1987.
- [12] C. D. Pirvu, A. Ortan, M. Hirjau, R. Prisada, D. Lupuleasa, and A. Bogdan, "Studies concerning the optimization of the pentoxifylline encapsulation," *Romanian Biotechnological Letters*, vol. 16, no. 1, pp. 66–73, 2011.
- [13] P. Matricardi, C. di Meo, T. Coviello, W. E. Hennink, and F. Alhaique, "Interpenetrating polymer networks polysaccharide hydrogels for drug delivery and tissue engineering," *Advanced Drug Delivery Reviews*, vol. 65, pp. 1172–1187, 2013.
- [14] P. Yang, Z. Quan, L. Lu, S. Huang, and J. Lin, "Luminescence functionalization of mesoporous silica with different morphologies and applications as drug delivery systems," *Biomaterials*, vol. 29, no. 6, pp. 692–702, 2008.
- [15] M. Carbone and R. Caminiti, "Fragmentation pathways of acetic acid upon adsorption on Si(1 0 0)2 × 1," *Surface Science*, vol. 602, no. 4, pp. 852–858, 2008.
- [16] E. Duguet, M. Treguer-Delapierre, and M.-H. Delville, "Functionalisation of inorganic nanoparticles for biomedical applications," in *Nanosciences: Nanobiotechnology and Nanobiology*, P. Boisseau, P. Houdy, and M. Lahmani, Eds., Springer, Berlin, Germany, 2009.
- [17] H. Ryssel, O. Kloeters, G. Germann, T. Schäfer, G. Wiedemann, and M. Oehlbauer, "The antimicrobial effect of acetic acid—an alternative to common local antiseptics?" *Burns*, vol. 35, no. 5, pp. 695–700, 2009.
- [18] C. J. Brinker and G. W. Scherer, *Sol-Gel Science: The Physics and Chemistry of Sol-Gel Processing*, chapter 2, Academic Press, New York, NY, USA, 1990.
- [19] D. P. Zarubin, "The two-component bands at about 4500 and 800 cm⁻¹ in infrared spectra of hydroxyl-containing silicas. Interpretation in terms of Fermi resonance," *Journal of Non-Crystalline Solids*, vol. 286, no. 1-2, pp. 80–88, 2001.
- [20] B. M. Rahman, M. A. Islam, M. I. I. Wahed et al., "In-vitro studies of pentoxifylline controlled-release from hydrophilic matrices," *Journal of Scientific Research*, vol. 1, no. 2, pp. 353–362, 2009.
- [21] S. Tamizharasi, J. C. Rathi, and V. Rathi, "Formulation, and evaluation of pentoxifylline-loaded poly(ϵ -caprolactone) microspheres," *Indian Journal of Pharmaceutical Sciences*, vol. 70, no. 3, pp. 333–337, 2008.
- [22] A. H. de Oliveira, E. A. de Moura, M. F. Pinto et al., "Thermal characterization of raw material pentoxifylline using thermo-analytical techniques and Pyr-GC/MS," *Journal of Thermal Analysis and Calorimetry*, vol. 106, no. 3, pp. 763–766, 2011.
- [23] J. Sun, Y. Li, L. Li et al., "Functionalization and bioactivity in vitro of mesoporous bioactive glasses," *Journal of Non-Crystalline Solids*, vol. 354, no. 32, pp. 3799–3805, 2008.
- [24] M. Fleisher, V. Stonkus, I. Liepina et al., "Theoretical study of ketonization reaction mechanism of acetic acid over SiO₂," in *Proceedings of the 13th International Electronic Conference on Synthetic Organic Chemistry (ECSOC '09)*, Riga, Latvia, November 2009.
- [25] J. Zhang, Z. Guo, X. Zhi, and H. Tang, "Surface modification of ultrafine precipitated silica with 3-methacryloxypropyltrimethoxysilane in carbonization process," *Colloids and Surfaces A: Physicochemical and Engineering Aspects*, vol. 418, no. 5, pp. 174–179, 2013.



Hindawi

Submit your manuscripts at
<http://www.hindawi.com>

